Anesthesiology 2008; 109:426–35

Direct Assessments of the Antioxidant Effects of Propofol Medium Chain Triglyceride/Long Chain Triglyceride on the Brain of Stroke-prone Spontaneously Hypertensive Rats Using Electron Spin Resonance Spectroscopy

Kyo Kobayashi, D.D.S., Fumihiko Yoshino, D.D.S., Ph.D.,† Shun-Suke Takahashi, D.D.S., Ph.D.,‡ Kazuo Todoki, Ph.D.,‡ Yojiro Maehata, D.D.S., Ph.D.,† Tomoko Komatsu, D.D.S., Ph.D.,§ Kazu-Ichi Yoshida, D.D.S., Ph.D.,‖ Masaichi-Chang-Il Lee, D.D.S., Ph.D.#*

Background: **Antioxidant anesthetics such as propofol (2,6-diisopropylphenol) directly inhibit lipid peroxidation *via* the generation of reactive oxygen species. Currently, there are no other studies regarding the direct effects of propofol medium chain triglyceride/long chain triglyceride (MCT/LCT) on reactive oxygen species generation or in experimental models of reactive oxygen species–induced oxidative stress in the brain.**

Methods: **The authors investigated the effects of propofol MCT/LCT on reactive oxygen species (hydroxyl radical or superoxide) by electron spin resonance spin trapping with 5,5-dimethyl-1-pyrroline-*N*-oxide. The effects of propofol MCT/LCT on oxidative stress in the brain of Wistar-Kyoto rats or stroke-prone spontaneously hypertensive rats were investigated by using an *in vivo* L-band electron spin resonance system to monitor the decay rate of 3-methoxycarbonyl-2,2,5,5-tetramethyl-pyrrolidine-1-oxyl as a nitroxyl spin probe.**

Results: **These studies provided direct evidence that propofol MCT/LCT inhibited hydroxyl radical generation, but not superoxide generation. Regarding the hydroxyl radical from the Fenton system, it is likely to be due to the scavenging effects of vehicle. Anesthesia with propofol MCT/LCT reduced the degree of the high oxidative stress in the brain of stroke-prone spontaneously hypertensive rats.**

Conclusion: **The current data show that propofol, mixed with clinical reagents (propofol MCT/LCT), resulted in the down-regulation of high oxidative stress due to scavenging hydroxyl radical, as demonstrated by *in vitro* or *in vivo* electron spin resonance analysis. These results led to reduced levels of hydroxyl radical, formed by brain injury such as stroke, and may therefore provide advantages for neuroprotection during anesthesia for craniotomy, *e.g.*, in cases of brain disease.**

IT has been reported that oxidative stress induced by reactive oxygen species (ROS) such as the hydroxyl radical ($HO^{\cdot}$) or superoxide ($O_2^{\cdot -}$) could be involved in various brain dysfunctions, including ischemia–reperfusion injury,[1] brain tumor,[2] aging,[3] familial amyotrophic lateral sclerosis,[4] Alzheimer disease,[5] and other neurodegenerative diseases.[6] The protective effects of general anesthetics in the brain are well known.[7–9] Moreover, antioxidant anesthetics, such as propofol (2,6-diisopropylphenol), inhibit lipid peroxidation *via* the generation of ROS.[7–9] Recently, it has been reported that antioxidant anesthetics reduce ischemia–reperfusion injury of the brain *via* their antioxidant property.[10,11]

During the past decade, it has become well accepted that propofol is an intravenous sedative–hypnotic agent popular for sedation within the intensive care unit.[12] The rapid recovery of patients after stopping propofol treatment makes it an attractive option for the intensive care unit, particularly for patients requiring only short-term sedation. One distinct advantage is the overall reduction in medical costs.[13] However, there are potential risks related to propofol treatment that need to be taken into consideration, such as increased serum triglyceride levels after long-term application.[13,14] Hypertriglyceridemia is one of the unwanted effects likely to occur during long-term propofol sedation using a formulation containing long chain triglycerides (LCTs) extracted from soybean oil. Recently, it has been reported that the use of propofol that has been formulated in a solvent consisting of medium chain triglycerides (MCTs) and LCT (MCT/LCT) might reduce the risk of hypertriglyceridemia.[15] It has also been reported that propofol has distinct antioxidant properties, because the chemical structure of propofol is similar to that of phenol-based ROS scavengers such as vitamin E.[16] However, no other study has specifically investigated the direct effects of propofol MCT/LCT on ROS generation or on experimental models of ROS-induced oxidative stress in the brain.

We previously developed an electron spin resonance (ESR)–based technique for the detection of free radical reactions, including ROS, in biologic systems.[17–22] Nitroxyl radicals are very useful as exogenous spin probes for measuring free radical distribution, oxygen concentration, and redox metabolism by *in vivo* ESR in biologic systems.[20–23] It has been reported that nitroxyl radicals, referred to as a "nitroxyl spin probe," lose their paramagnetism through a redox reaction when exposed to a reducing agent in biologic systems.[24,25] The signal decay rate of the nitroxyl spin probe provides evidence of ROS generation and changes of redox status in biologic systems.[26,27]

* Graduate Student, ‖ Professor, Department of Clinical Care Medicine, Division of Anesthesiology, § Assistant Professor, Division of Dentistry for Special Patients, † Research Assistant, ‡ Assistant Professor, # Professor, Division of Pharmacology and ESR (Electron Spin Resonance) Laboratories, Kanagawa Dental College.

Received from Kanagawa Dental College, Yokosuka, Kanagawa, Japan. Submitted for publication June 4, 2007. Accepted for publication April 17, 2008. Supported by grants from the High-Tech Research Center Project of Kanagawa Dental College, Yokosuka, Kanagawa, Japan (to Drs. Kobayashi, Yoshino, Takahashi, Todoki, Maehata, and Prof. Lee), and Grants-in-Aid for Scientific Research from the Japanese Ministry of Education, Science, and Culture, Tokyo (to Drs. Yoshino [16791169], Maehata [18890213], and Komatsu and Lee [19592371]).

Address correspondence to Dr. Lee: Department of Clinical Care Medicine, Division of Pharmacology and ESR Laboratories, Kanagawa Dental College, Yokosuka, Kanagawa, Japan. ieeman@kdcnet.ac.jp.

The stroke-prone spontaneously hypertensive rat (SHRSP), a model of essential stroke, has several characteristics of increased oxidative stress.[21,22,28,29] This has led to the technique being described as involving the blood-brain barrier–permeable nitroxyl spin probe 3-methoxycarbonyl-2,2,5,5-tetramethylpyrrolidine-1-oxyl (MC-PROXYL) for the assessment of oxidative stress in the brain.[20–22] Furthermore, these results suggest that MC-PROXYL is a suitable spin probe for ESR detection of free radical reactions in the brain of rodent models. In the current study, we investigated the effect of propofol MCT/LCT, including an appropriate vehicle such as MCT/LCT, on the scavenging effects of ROS and the decay rate constants of MC-PROXYL in the SHRSP brain by ESR techniques. These studies showed that propofol MCT/LCT could reduce ROS-induced oxidative stress in the brain of the SHRSP due to scavenging $HO^{\cdot}$.

Materials and Methods

Reagents

Propofol MCT/LCT (1% propofol injection, Maruishi) was purchased from Maruishi Pharmaceutical (Osaka, Japan). MCT/LCT was prepared with soybean oil, MCT, lecithin from chicken eggs, glycerol, and sodium oleate. Propofol LCT (1% Diprivan injection) was purchased from AstraZeneca Ltd. (Osaka, Japan). Xanthine oxidase (XO) (grade III: from buttermilk, chromatographically purified suspension in 2.3 M $(NH_4)_2SO_4$, 10 mM sodium phosphate buffer [pH 7.8], containing 1 mM EDTA and 1 mM sodium salicylate), xanthine, and superoxide dismutase were obtained from Sigma (St. Louis, MO). Hydrogen peroxide (H_2O_2) and $FeSO_4$ were obtained from Wako Chemical (Osaka, Japan). 5,5-Dimethyl-1-pyrroline-*N*-oxide (DMPO) was purchased from Labotec (Tokyo, Japan). MC-PROXYL was synthesized from 3-carboxy-2,2,5,5-tetramethyl-pyrrolidine-1-oxyl (carboxy-PROXYL; Tokyo Kasei, Tokyo, Japan) and diazomethane (Wako Chemical) was synthesized by a method described previously.[20–22]

In Vitro *ESR Measurement*

$HO^{\cdot}$ were generated by the Fenton reaction (H_2O_2 plus $FeSO_4$) as described previously.[30,31] $HO^{\cdot}$ were generated by ultraviolet irradiation of H_2O_2 as described previously.[32,33] $O_2^{\cdot-}$ were generated by the xanthine–XO system by methods also described previously.[18] All solutions were prepared in 0.1 M phosphate-buffered saline (pH 7.2). ESR spin trapping was conducted with a ROS generating system containing DMPO. ESR observations were performed with a JES-RE 3X, X-band spectrometer (JEOL, Tokyo, Japan) connected to a WIN-RAD ESR Data Analyzer (Radical Research, Tokyo, Japan) at the following instrument settings: microwave power, 8.00 mW; magnetic field, 335.638 ± 5 mT; field modulation width, 0.079 mT; receiver gain, 400; sweep time, 1 min; and time constant, 0.03 s. Hyperfine coupling constants were calculated based on resonance frequency, measured with a microwave frequency counter, and resonance field, measured with a JEOL ES-FC5 field measurement unit. To quantify the spin adducts detected, we obtained ESR spectra for manganese oxide standards. After the ESR spectra were recorded, the signal intensity, expressed as relative height, was normalized against the signal intensity of the manganese oxide standard.[30,31] All experiments were repeated a minimum of four times.

In Vivo *ESR Measurement*

The procedures used in this study were in accordance with the guidelines of the US National Institutes of Health *Guide for the Care and Use of Laboratory Animals* (publication 85-23, revised 1985), and our protocols were approved by Animal Care Committees of Kanagawa Dental College (Yokosuka, Japan). Male Wistar-Kyoto rats (WKYs) and SHRSPs, weighing approximately 100–120 g, were purchased from Japan SLC (Hamamatsu, Japan).

In preliminary experiments, we confirmed that WKYs and SHRSPs were successfully anesthetized with a minimal concentration of pentobarbital (30 mg/kg, intravenous) for *in vivo* L-band ESR. Therefore, WKYs and SHRSPs were anesthetized with pentobarbital (30 mg/kg, intravenous) or propofol MCT/LCT (20 mg/kg, intravenous) and used for *in vivo* L-band ESR. We then analyzed the head region of WKYs or SHRSPs with *in vivo* L-band ESR analysis as described previously.[21,22] The ESR spectra from SHRSPs were obtained with a L-band ESR spectrometer (JES-RE-3 l; JEOL, Akishima, Japan) equipped with a four-window loop-gap resonator, under the following conditions: microwave power, 10 mW; magnetic field, 50.0 ± 10 mT; field modulation width, 1 mT; receiver gain, 79–320; sweep time, 0.5 min; and time constant, 0.03 s. All experiments were repeated a minimum of five times.

Measurement of Cerebral Blood Flow

The decay rate of MC-PROXYL was used, under the same conditions as the L-band ESR assay, to ascertain whether propofol MCT/LCT treatment had any effect on cerebral blood flow (CBF) in the brain of SHRSPs and WKYs. CBF was measured by a laser Doppler flowmeter (TBF-LN1; Unique Medical, Tokyo, Japan) using a laser Doppler flowmetry probe (LP-C; Unique Medical). It has previously been reported that urethane anesthetic has a wide safety margin and has little influence on normal blood pressure and the general circulation.[34,35] As a consequence, rats were anesthetized with urethane (1.2 g/kg, intraperitoneal) before CBF measurements. Each rat was fixed on a wooden board (18 × 25 cm) in the prone position. All limbs were fixed at an angle of 45° to the body midline with adhesive tape. The head was also fixed to the board with adhesive tape. A laser

Doppler flowmetry probe was glued directly onto the surface of the skull. The output signals from the flowmeter were recorded on a computer hard disk through an analog–digital converter and displayed simultaneously on the monitor. CBF was recorded and analyzed using data analysis software (Chart version 4.2; AD Instruments, Inc., Colorado Springs, CO). After CBF had stabilized at a baseline, propofol MCT/LCT (20 mg/kg) was administered by tail vein injection. CBF was then continuously monitored over a 10-min period, the same time course as L-band ESR studies. Pericranial temperature, arterial oxygen tension, arterial carbon dioxide tension, and blood pressure were controlled and remained at consistent levels across all groups before or during CBF measurements. All of the traces presented are typical results. All experiments were repeated a minimum of four times.

Statistical Analysis

Statistical analyses were performed using Statcel (OMS, Saitama, Japan). Analyses demonstrated that data arising from this experiment were normally distributed. Results are presented as mean ± SD. Two-way analysis of variance was used to compare the averages of six concentration levels and between agents. The Bonferroni/Dunn test was used for multiple comparisons. Regression analysis was applied to data obtained from the L-band ESR analysis. The Student *t* test was used to compare averages between WKY and SHRSP. A *P* value of less than 0.05 was considered to be statistically significant.

Results

Effects of Propofol MCT/LCT on HO· Generation by the Fenton System

In the current study, we investigated the effects of propofol MCT/LCT on HO·, which had been generated from the Fenton reaction, by ESR spin trapping with DMPO.

As reported previously,[30,31,36] after the addition of H_2O_2 to $FeSO_4$, we primarily observed a characteristic DMPO-OH spin adduct spectrum with hyperfine splitting giving rise to four resolved peaks (figs. 1A and B, control). With propofol MCT/LCT (56.09–5,609 μM) pretreatment of $FeSO_4$ and subsequent addition of H_2O_2, it was apparent that the DMPO-OH signal was reduced in a

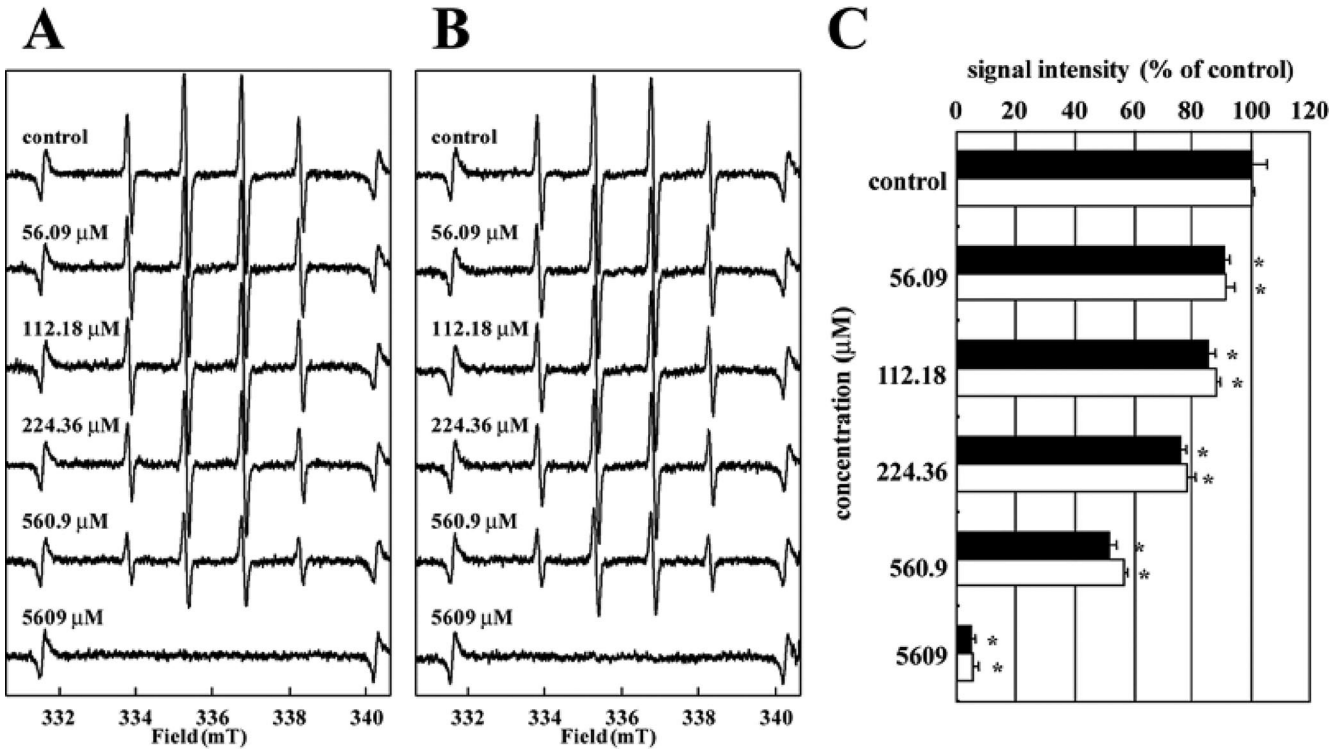

Fig. 1. Effects of propofol medium chain triglyceride/long chain triglyceride (MCT/LCT) or vehicle on hydroxyl radical (HO·) generation from the Fenton reaction. (*A*) Electron spin resonance spin trapping measurement of HO· generation from H_2O_2 (20 μM) and $FeSO_4$ (20 μM) in 0.1 M phosphate-buffered saline (pH 7.2) as spin trap 5,5-dimethyl-1-pyrroline-*N*-oxide (DMPO; 50 mM) in the absence of propofol MCT/LCT (control) with propofol MCT/LCT pretreatment at 56.09 μM, 112.18 μM, 224.36 μM, 560.9 μM, and original liquid (5,609 μM), respectively. (*B*) Electron spin resonance spin trapping measurement of HO· generation from H_2O_2 (20 μM) and $FeSO_4$ (20 μM) in 0.1 M phosphate-buffered saline (pH 7.2) as spin trap DMPO (50 mM) in the absence of vehicle (MCT/LCT) (control) with equivalent vehicle (MCT/LCT) pretreatment of propofol MCT/LCT. Signals appearing at either side of the electron spin resonance spectra correspond to manganese oxide installed in the cavity as a reference. In *C*, we report the dose–response of propofol MCT/LCT (56.09–5,609 μM; *closed column*) or equivalent vehicle (*open column*) on HO· generation from the Fenton reaction. The signal intensity of the second peak of the spectrum was normalized as the relative height against the standard's signal intensity of the manganese oxide marker. Data are presented as mean ± SD of quadruplicate experiments. * Significantly different ($P < 0.05$) from the corresponding control value.

dose-dependent manner (fig. 1A). However, with pretreatment using the equivalent vehicle (MCT/LCT), it was also demonstrated that the DMPO-OH signal was reduced in a dose-dependent manner (fig. 1B). These data indicate that, within this system, propofol MCT/LCT markedly inhibits $HO^{\cdot}$ generation from the Fenton reaction as a result of scavenging, both by the propofol MCT/LCT and by the vehicle. It was also clear that both propofol MCT/LCT and the vehicle reduced $HO^{\cdot}$ generation in a dose-dependent manner (fig. 1C).

Effects of Propofol MCT/LCT on $HO^{\cdot}$ Generation by Ultraviolet Irradiation of H_2O_2

In the next study, we investigated the effects of propofol MCT/LCT on $HO^{\cdot}$, which had been generated from ultraviolet irradiation of H_2O_2, and by ESR spin trapping with DMPO.

As reported previously,[32,33,36] after ultraviolet irradiation of H_2O_2, we primarily observed a characteristic DMPO-OH spin adduct spectrum with hyperfine splitting giving rise to four resolved peaks (figs. 2A and B, control). When H_2O_2 was pretreated with propofol MCT/LCT (56.09–5,609 μM) followed by ultraviolet irradiation, it was apparent that the DMPO-OH signal was reduced in a dose-dependent manner (fig. 2A). When the experiment was repeated using the equivalent vehicle pretreatment, it was evident that the DMPO-OH signal was not significantly different at low concentration (figs. 2B and C) but was reduced at high concentrations (>560.09 μM) of vehicle (figs. 2B and C). Interestingly, the inhibitory effects of propofol MCT/LCT (>224.36 μM) were significant stronger than the vehicle alone (fig. 2C). These data suggest that propofol MCT/LCT directly inhibited $HO^{\cdot}$ generation in a manner that was independent of the scavenging effects of the vehicle (fig. 2C).

Effects of Propofol MCT/LCT and Propofol LCT on $HO^{\cdot}$ Generation by the Fenton System

In the current study, we investigated the effects of other propofol formulations, such as propofol LCT (Diprivan) on $HO^{\cdot}$ generated from the Fenton reaction by ESR spin trapping with DMPO.

When $FeSO_4$ was pretreated with propofol MCT/LCT (56.09–5,609 μM) and the subsequent addition of H_2O_2, it

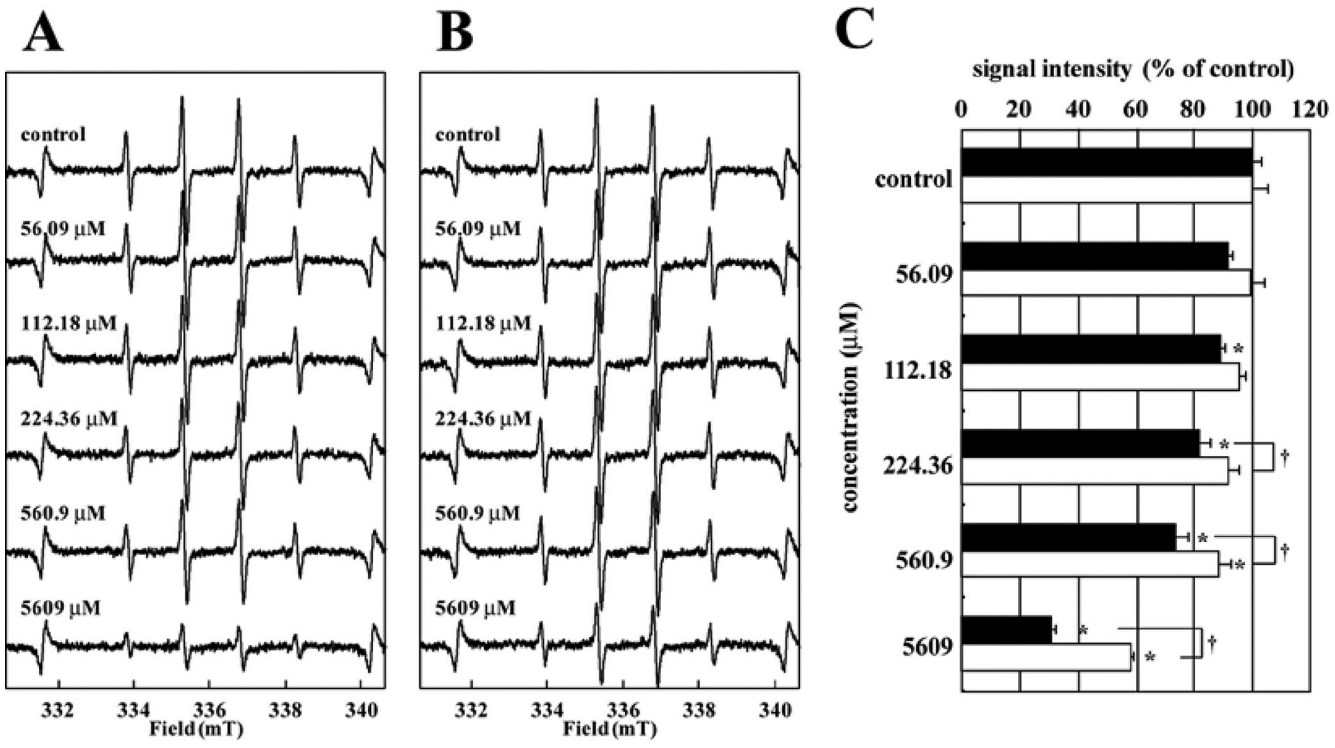

Fig. 2. Effects of propofol medium chain triglyceride/long chain triglyceride (MCT/LCT) or vehicle on the generation of hydroxyl radical ($HO^{\cdot}$) from ultraviolet irradiation of H_2O_2. (*A*) Electron spin resonance spin trapping measurement of $HO^{\cdot}$ generation from ultraviolet irradiation (365 nm, 40 mW) of H_2O_2 (20 mM) in 0.1 M phosphate-buffered saline (pH 7.2) as spin trap 5,5-dimethyl-1-pyrroline-*N*-oxide (DMPO; 50 mM) in the absence of propofol MCT/LCT (control) with propofol MCT/LCT pretreatment at 56.09 μM, 112.18 μM, 224.36 μM, 560.9 μM, and original liquid (5,609 μM), respectively. (*B*) Electron spin resonance spin trapping measurement of $HO^{\cdot}$ generation from ultraviolet irradiation of H_2O_2 in 0.1 M phosphate-buffered saline (pH 7.2) as spin trap DMPO (50 mM) in the absence of vehicle (MCT/LCT) (control) with equivalent vehicle (MCT/LCT) pretreatment of propofol MCT/LCT. Signals appearing at either side of the electron spin resonance spectra correspond to manganese oxide installed in the cavity as a reference. In *C*, we present the dose–response of propofol MCT/LCT (56.09–5,609 μM; *closed column*) or equivalent vehicle (*open column*) on $HO^{\cdot}$ generation *via* ultraviolet irradiation of H_2O_2. The signal intensity of the second peak of the spectrum was normalized as the relative height against the standard's signal intensity of the manganese oxide marker. Data are presented as mean ± SD of quadruplicate experiments. * Significantly different ($P < 0.05$) from the corresponding control value. † Significantly different ($P < 0.05$) from the corresponding value of the MCT/LCT vehicle.

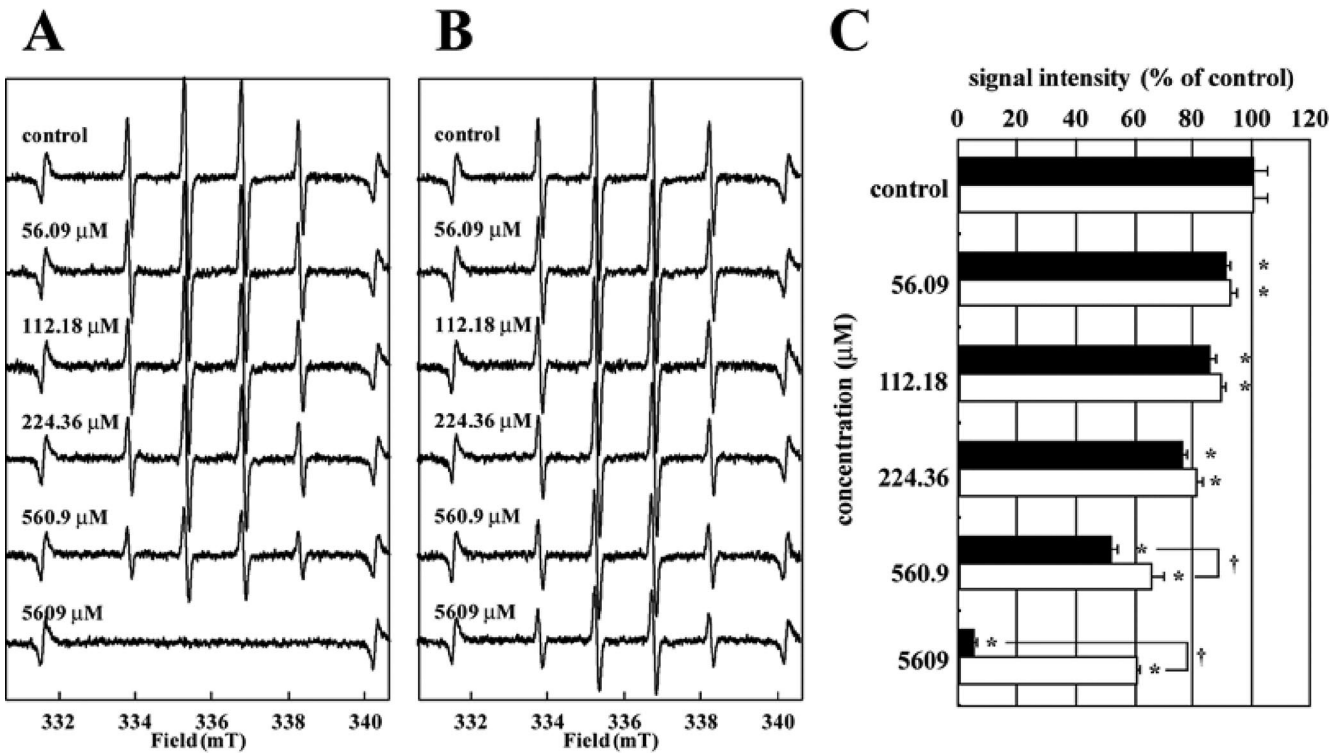

Fig. 3. Effects of propofol medium chain triglyceride/long chain triglyceride (MCT/LCT) or propofol LCT (Diprivan) on hydroxyl radical ($HO^{\cdot}$) generation from the Fenton reaction. (*A*) Electron spin resonance spin trapping measurement of $HO^{\cdot}$ generation from H_2O_2 (20 μM) and $FeSO_4$ (20 μM) in 0.1 M phosphate-buffered saline (pH 7.2) as spin trap 5,5-dimethyl-1-pyrroline-*N*-oxide (DMPO; 50 mM) in the absence of propofol MCT/LCT (control) with propofol MCT/LCT pretreatment at 56.09 μM, 112.18 μM, 224.36 μM, 560.9 μM, and original liquid (5,609 μM), respectively. (*B*) Electron spin resonance spin trapping measurement of $HO^{\cdot}$ generation from H_2O_2 (20 μM) and $FeSO_4$ (20 μM) in 0.1 M phosphate-buffered saline (pH 7.2) as spin trap DMPO (50 mM) in the absence of vehicle (MCT/LCT) (control) with equivalent vehicle (MCT/LCT) pretreatment of propofol MCT/LCT. Signals appearing at either side of the electron spin resonance spectra correspond to manganese oxide installed in the cavity as a reference. In *C*, we present the dose–response of propofol MCT/LCT (56.09–5,609 μM; *closed column*) or propofol LCT (56.09–5,609 μM; *open column*) on $HO^{\cdot}$ generation from the Fenton reaction. The signal intensity of the second peak of the spectrum was normalized as the relative height against the standard's signal intensity of the manganese oxide marker. Data are presented as mean ± SD of quadruplicate experiments. * Significantly different ($P < 0.05$) from the corresponding control value. † Significantly different ($P < 0.05$) from the corresponding value of propofol LCT.

was apparent that the DMPO-OH signal was reduced in a dose-dependent manner (fig. 3A), as shown in figure 1. With equivalent propofol LCT (56.09–5,609 μM) pretreatment, it was also shown that the DMPO-OH signal was reduced in a dose-dependent manner (fig. 3B). We also observed that the inhibitory effects of a high concentration of propofol MCT/LCT (>560.9 μM) were significantly stronger than propofol LCT (fig. 3C). Collectively, these data strongly indicate that, within this system, the vehicle can account for the scavenging effects of $HO^{\cdot}$ on the concentration of propofol MCT/LCT (fig. 1C).

Effects of Propofol MCT/LCT and Propofol LCT on $HO^{\cdot}$ Generation by Ultraviolet Irradiation of H_2O_2

In the next study, we also investigated the effects of propofol LCT on $HO^{\cdot}$ generated from ultraviolet irradiation of H_2O_2 and ESR spin trapping with DMPO.

As shown in figure 2, with propofol MCT/LCT (56.09–5,609 μM) pretreatment of H_2O_2 and subsequent ultraviolet irradiation, it was apparent that the DMPO-OH signal was reduced in a dose-dependent manner (fig. 4A). With equivalent propofol LCT pretreatment, it was also shown that the DMPO-OH signal was reduced in a dose-dependent manner (fig. 4B). The inhibitory effects of propofol MCT/LCT were no different in propofol LCT (fig. 4C). These data suggest that propofol LCT can also inhibit $HO^{\cdot}$ generation directly (fig. 4C), in a manner similar to that propofol MCT/LCT (fig. 2C).

Effects of Propofol MCT/LCT on $O_2^{\cdot-}$ Generation

We also investigated the effects of propofol MCT/LCT on XO-mediated $O_2^{\cdot-}$ generation, as measured by ESR spin trapping with DMPO. As reported previously,[36] after addition of xanthine to XO, we primarily observed a characteristic DMPO-OOH adduct spectrum with hyperfine splitting giving rise to 12 resolved peaks (fig. 5A, a). These signals were quenched by 150 U/ml superoxide dismutase, thus confirming that they were derived from $O_2^{\cdot-}$ (fig. 5A, b). With propofol MCT/LCT (original liquid; 5,609 μM) pretreatment of XO and subsequent addition of xanthine, however, we did not observe any alterations in

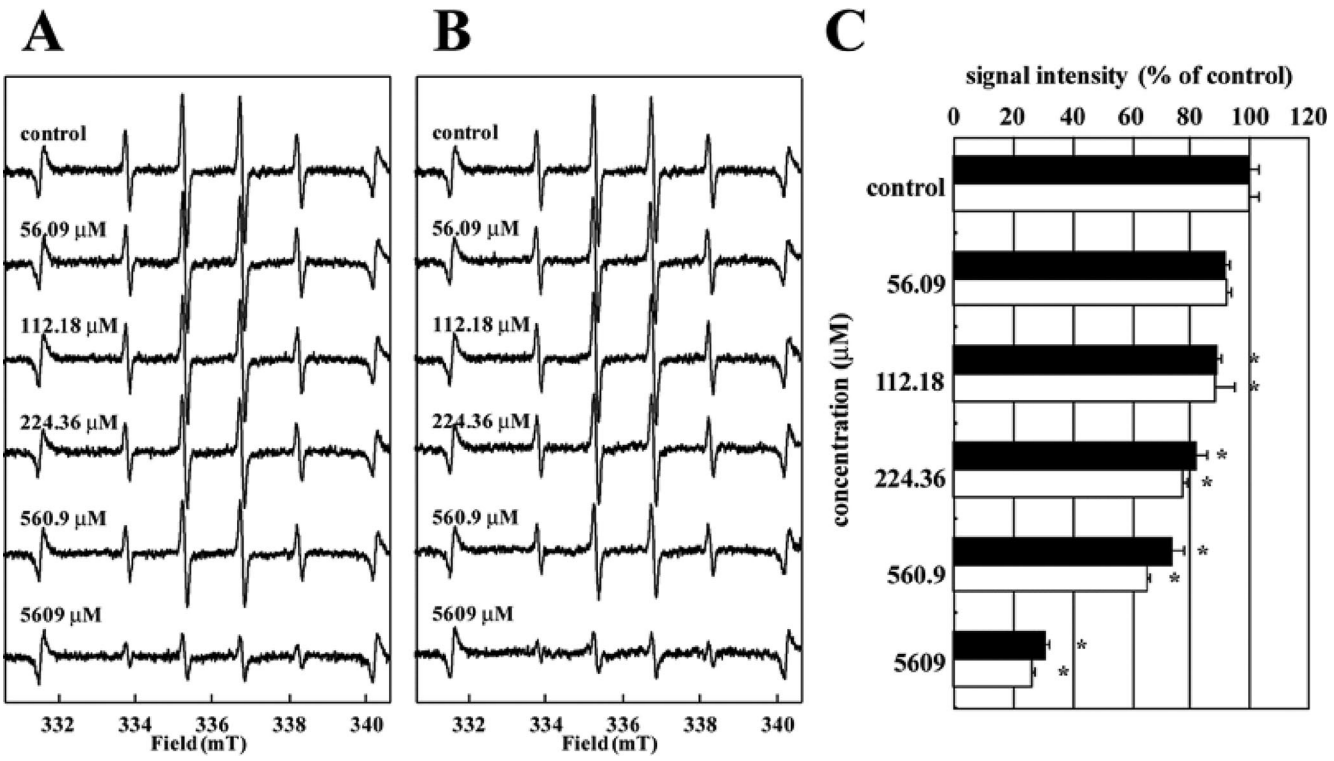

Fig. 4. Effects of propofol medium chain triglyceride/long chain triglyceride (MCT/LCT) or propofol LCT (Diprivan) on the generation of hydroxyl radical ($HO^{\cdot}$) from ultraviolet irradiation of H_2O_2. (*A*) Electron spin resonance spin trapping measurement of $HO^{\cdot}$ generation from ultraviolet irradiation (365 nm, 40 mW) of H_2O_2 (20 mM) in 0.1 M phosphate-buffered saline (pH 7.2) as spin trap 5,5-dimethyl-1-pyrroline-*N*-oxide (DMPO; 50 mM) in the absence of propofol MCT/LCT (control) with propofol MCT/LCT pretreatment at 56.09 μM, 112.18 μM, 224.36 μM, 560.9 μM, and original liquid (5,609 μM), respectively. (*B*) Electron spin resonance spin trapping measurement of $HO^{\cdot}$ generation *via* ultraviolet irradiation of H_2O_2 in 0.1 M phosphate-buffered saline (pH 7.2) as spin trap DMPO (50 mM) in the absence of vehicle (MCT/LCT) (control) with equivalent vehicle (MCT/LCT) pretreatment of propofol MCT/LCT. Signals appearing at either side of the electron spin resonance spectra correspond to manganese oxide installed in the cavity as a reference. In *C*, we present the dose–response of propofol MCT/LCT (56.09–5,609 μM; *closed column*) or propofol LCT (56.09–5,609 μM; *open column*) on $HO^{\cdot}$ generation *via* ultraviolet irradiation of H_2O_2. The signal intensity of the second peak of the spectrum was normalized as the relative height against the standard's signal intensity of the manganese oxide marker. Data are presented as mean ± SD of quadruplicate experiments. * Significantly different ($P < 0.05$) from the corresponding control value.

the ESR spectrum, which exhibited identical DMPO-OOH spin adducts (fig. 5A, c). Data showed that propofol MCT/LCT had no effect on $O_2^{\cdot-}$ generation from xanthine–XO in this system (fig. 5B).

Effects of Propofol MCT/LCT on SHRSP-induced Oxidative Stress in the Brain

The effects of propofol MCT/LCT on SHRSP-induced oxidative stress in the brain were investigated using an

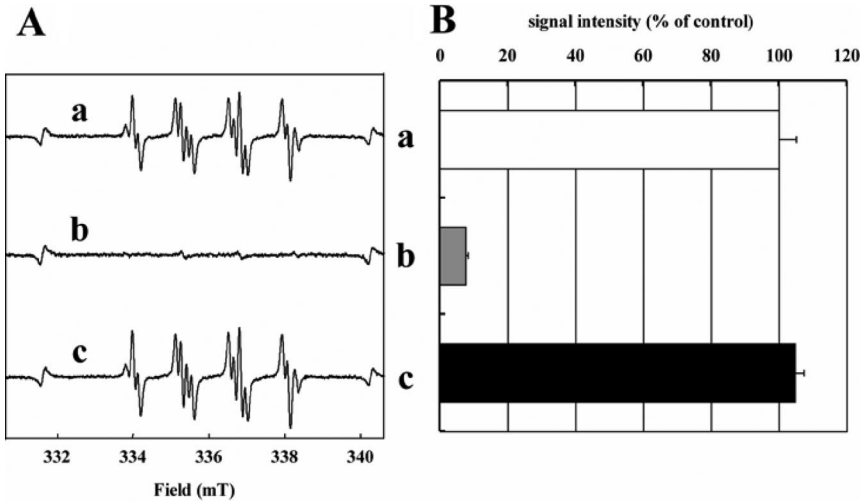

Fig. 5. Effects of propofol medium chain triglyceride/long chain triglyceride (MCT/LCT) on superoxide ($O_2^{\cdot-}$) generation. (*A*) Electron spin resonance spin trapping measurement of $O_2^{\cdot-}$ generation from xanthine oxidase (0.1 U/ml) and xanthine (362 μM) in 0.1 M phosphate-buffered saline (pH 7.2) as spin trap 5,5-dimethyl-1-pyrroline-*N*-oxide (440 mM) (*a*) in the absence of propofol MCT/LCT (control) (*b*) with pretreatment of superoxide dismutase (150 U/ml) to xanthine oxidase (*c*) with propofol MCT/LCT pretreatment (original liquid; 5,609 μM). Signals appearing at either side of the electron spin resonance spectra correspond to manganese oxide installed in the cavity as a reference. In *B*, we report the effects of propofol MCT/LCT (original liquid; 5,609 μM) on $O_2^{\cdot-}$ generation from xanthine oxidase and xanthine. The signal intensity of the second peak of the spectrum was normalized as the relative height against the standard's signal intensity of the manganese oxide marker. Data are presented as mean ± SD of quadruplicate experiments.

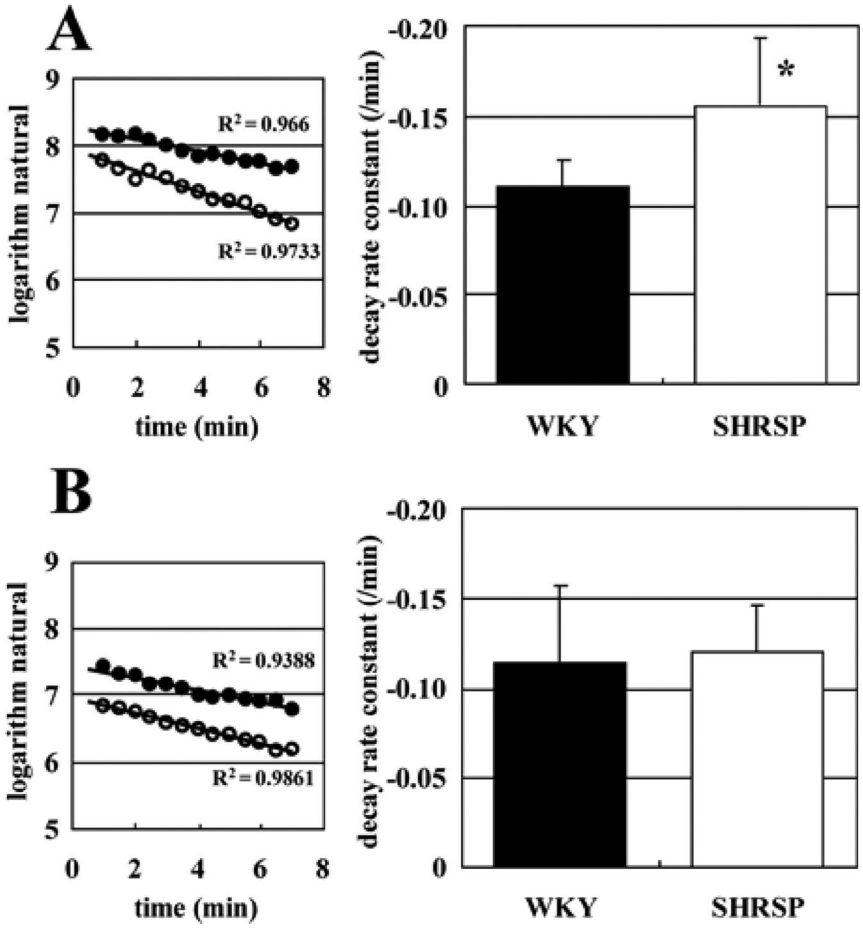

Fig. 6. Effects of propofol medium chain triglyceride/long chain triglyceride (MCT/LCT) on stroke-prone spontaneously hypertensive rat (SHRSP)–induced oxidative stress in the brain. Rats were anesthetized with pentobarbital (30 mg/kg, intravenous) (*A*) and propofol MCT/LCT (20 mg/kg, intravenous) (*B*). L-band electron spin resonance was used to determine the signal decay of 3-methoxycarbonyl-2,2,5,5-tetramethyl-pyrrolidine-1-oxyl (MC-PROXYL) in the head region of live Wistar-Kyoto rats (WKYs) and SHRSPs after intravenous injection of MC-PROXYL. Rats were treated with MC-PROXYL (140 mM, 5 ml/kg) *via* the tail vein, and electron spin resonance spectra were measured within the head region of live rats. The logarithmic signal intensity of the second peak within the electron spin resonance spectrum of the nitroxyl spin probes was plotted against time. (*Inset*) Regression line fitted to a typical plot of L-band ESR data. Data are presented as mean ± SD of WKYs (n = 5) or SHRSPs (n = 5) with pentobarbital and with propofol MCT/LCT. * Significance ($P < 0.05$) from the corresponding control value of the WKYs.

in vivo L-band system to monitor the decay rate of MC-PROXYL as a nitroxyl spin probe. The decay rate constants of MC-PROXYL were significantly greater in the head region of SHRSPs than in WKYs anesthetized with pentobarbital (30 mg/kg, intravenous) (fig. 6A). Furthermore, the decay rate constant of SHRSPs was significantly faster than in WKYs, suggesting that oxidative stress in the brain of SHRSPs was higher compared with that in WKYs, the latter being the oxidative stress model reported in our previous study.[21,22] However, we did not observe any alterations in the decay rate constant of MC-PROXYL in the head region of either SHRSPs or WKYs anesthetized with propofol MCT/LCT (20 mg/kg, intravenous) (fig. 6B). These results indicated that the induced oxidative stress in the SHRSP brain was reduced by propofol MCT/LCT but not by pentobarbital.

Effects of Propofol MCT/LCT on CBF in WKYs or SHRSPs

Figure 7 shows the typical effects of propofol MCT/LCT on CBF in WKYs (A) and SHRSPs (B). Upon propofol MCT/LCT administration, we observed a rapid decline in CBF, both in WKYs and in SHRSPs; CBF levels reached the same minimum level in the two models within a few seconds (figs. 7A and B). Furthermore, it was observed that there was no significant difference between the WKYs and SHRSPs when CBF levels were compared 10 min after propofol MCT/LCT injection (figs. 7A and B), equivalent to the period of time monitored in the L-band ESR study (fig. 6), although CBF levels in WKYs were higher than in SHRSPs immediately before the injection of propofol MCT/LCT (fig. 7C). These results indicated that anesthesia undertaken with propofol MCT/LCT during L-band ESR measurements had no significant effect on the levels of CBF in either WKYs or SHRSPs.

Discussion

Propofol anesthesia has been associated with lower intracranial pressure and cerebral swelling than volatile anesthesia in brain tumor patients undergoing craniotomy.[37,38] The potential neuroprotective effect of propofol may be mediated by its antioxidant properties, which have been shown to play a role in apoptosis, ischemia–reperfusion injury, and inflammatory-induced neuronal damage.[39,40] However, questions and controversy remain regarding whether propofol modulates ROS generation and ROS-induced oxidative stress in the brain. Many existing studies have assessed the antioxidant effects of propofol by measuring lipid peroxidation.[7–9] However, these previous studies do not demonstrate the direct effects of ROS generation.

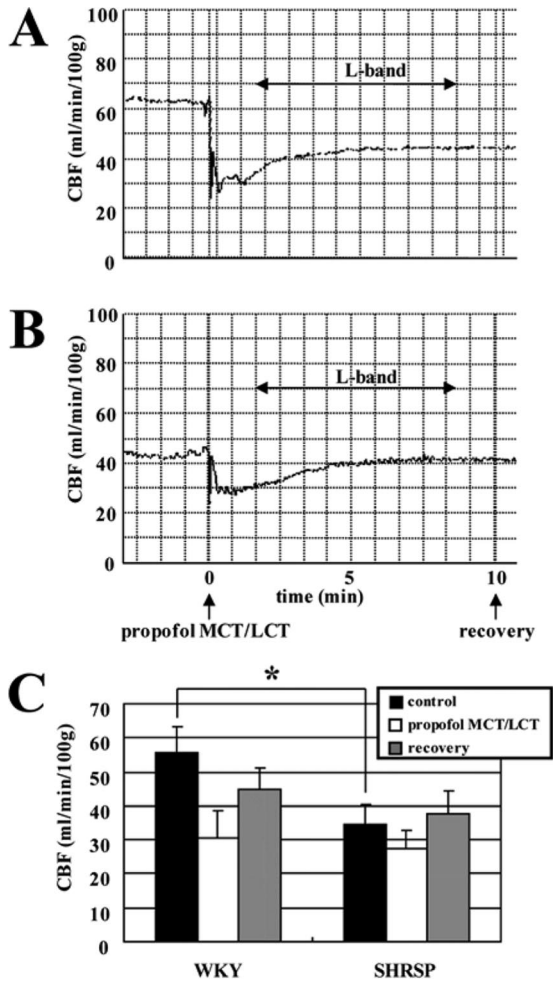

Fig. 7. Effects of propofol medium chain triglyceride/long chain triglyceride (MCT/LCT) on cerebral blood flow (CBF) in Wistar-Kyoto rats (WKYs) and stroke-prone spontaneously hypertensive rats (SHRSPs). Typical tracing of CBF in WKYs (*A*) and SHRSPs (*B*). After CBF had stabilized at a baseline, propofol MCT/LCT (20 mg/kg) was administered by tail vein injection. CBF was continuously monitored for a period of 10 min, the same time course as the L-band electron spin resonance studies. The *horizontal arrows* on each trace correspond to the time from the start and end of L-band electron spin resonance measurement. (*C*) Each column represents baseline CBF before propofol MCT/LCT administration (*closed columns*; control), minimum CBF within a few seconds of propofol administration (*open columns*; propofol MCT/LCT), and CBF 10 min after propofol MCT/LCT administration (*gray columns*; recovery) in WKYs and SHRSPs. The results are expressed as mean ± SD of WKYs (n = 4) or SHRSPs (n = 4). * Significance ($P < 0.05$) from the corresponding control values of WKYs and SHRSPs.

As a consequence, we have performed studies to assess the direct effects of ROS generation, such as $HO^{\cdot}$ and $O_2^{\cdot -}$, using ESR. Our studies provide direct evidence that propofol MCT/LCT inhibits $HO^{\cdot}$ generation but not $O_2^{\cdot -}$ generation from xanthine–XO (figs. 1–5).

First, we can confirm that propofol MCT/LCT inhibited the generation of $HO^{\cdot}$ from the Fenton reaction in a dose-dependent manner (figs. 1A and C). Surprisingly, the equivalent vehicle solution also reduced $HO^{\cdot}$ generation in a dose-dependent manner (figs. 1B and C) in this system. It is well established that $HO^{\cdot}$ can be generated from a reaction known as the biologic Fenton reaction.

$$Fe^{2+} + H_2O_2 \rightarrow Fe^{3+} + HO^{\cdot} + OH^{-}$$

The existence of this type of reaction in disease states was indicated by the ability of an iron chelator such as Desferal to reduce the high-intensity signal of the DMPO-OH spin adduct, thus suggesting the generation of $HO^{\cdot}$.[41,42] The generation of $HO^{\cdot}$ from the Fenton reaction has been shown to be a critical factor in various ROS-induced brain diseases.[43] Our current results provide the first direct evidence of the antioxidant properties of a vehicle such as MCT/LCT. The effects of the vehicle are most probably due to scavenging $HO^{\cdot}$ from the biologic Fenton reaction in tissues such as the brain. Further studies are urgently required to study how MCT/LCT scavenges $HO^{\cdot}$ generated *via* the Fenton reaction or ultraviolet irradiation of H_2O_2 *in vitro*. It would also be important to investigate how MCT/LCT scavenges $HO^{\cdot}$ from the brain of SHRSPs *in vivo*.

Second, we investigated the effect of propofol MCT/LCT on other $HO^{\cdot}$ generating systems using ultraviolet irradiation of H_2O_2, a well-known Fe^{2+}-independent reaction.[32,33] Interestingly, propofol MCT/LCT inhibited the generation of $HO^{\cdot}$ *via* ultraviolet irradiation of H_2O_2 in a dose-dependent manner (figs. 2A and C). An equivalent vehicle also reduced the generation of $HO^{\cdot}$ in a dose-dependent manner (figs. 2B and C) in this system, but the inhibitory effects observed were smaller than with propofol MCT/LCT (fig. 2C). These results suggested that the scavenging effects of propofol MCT/LCT on $HO^{\cdot}$ in this system would also be dependent on the effects of the vehicle. However, the high concentration of propofol MCT/LCT (> 224.36 μM) could be directly inhibited the $HO^{\cdot}$ generated by ultraviolet irradiation of H_2O_2.

Our next study was performed to compare the antioxidant characteristics of propofol MCT/LCT with other types of propofol in an LCT emulsion, propofol LCT (Diprivan), by measuring the $HO^{\cdot}$ generating system by use of the ESR technique. Propofol MCT/LCT inhibited the generation of $HO^{\cdot}$ *via* the Fenton system in a dose-dependent manner (figs. 3A and C). With the equivalent propofol LCT, we also observed a reduction in $HO^{\cdot}$ generation in a dose-dependent manner (figs. 3B and C), although the inhibitory effects were smaller than with propofol MCT/LCT (fig. 3C). The powerful effects of propofol MCT/LCT on the generation of $HO^{\cdot}$ *via* the Fenton system are likely to be caused by scavenging of the vehicle (fig. 1C). It is likely that a vehicle such as propofol LCT exerts smaller antioxidant effects compared with propofol MCT/LCT. In addition, propofol LCT also directly inhibited the generation of $HO^{\cdot}$ *via* ultraviolet irradiation of H_2O_2 system (fig. 4C) in a similar manner to propofol MCT/LCT (figs. 2 and 4). From these results, it is possible that the dual antioxidant properties

of propofol MCT/LCT would be stronger than those of propofol LCT alone, especially in terms of the biologic Fenton system. This is likely due to the scavenging effects of vehicle, such as MCT/LCT (fig. 1C).

Excellent and predictable recovery conditions, as well as minimal postoperative side effects, make propofol particularly suitable in awake craniotomies.[37,38] However, little is known about the potential effects of propofol on oxidative stress in the brain of *in vivo* experimental models. *In vivo* L-band ESR spectroscopy is a highly useful technique for the noninvasive investigation of redox status in living organisms. Our laboratories have previously reported that quantitative ESR analysis using MC-PROXYL has the potential to be highly useful for understanding redox status under conditions of oxidative stress in the rodent brain.[20–22] Severe hypertension and cerebrovascular diseases develop in SHRSPs.[44] ROS generation occurs after reperfusion, and this ROS-induced oxidative stress can greatly damage neurons in SHRSPs.[45] We evaluated high oxidative stress in the brain of SHRSPs using *in vivo* L-band ESR.[21,22] Consequently, it is clear from our SHRSP investigations that ESR techniques are highly useful in the assessment of the antioxidant properties of propofol MCT/LCT for use clinically. Indeed, we confirmed that oxidative stress in the brain of SHRSPs was higher compared with that in WKYs anesthetized with pentobarbital (fig. 6A). When propofol MCT/LCT was used as an anesthetic, rather than pentobarbital, the level of oxidative stress in SHRSPs became similar to that seen in WKYs (fig. 6B), suggesting that propofol MCT/LCT reduced SHRSP-induced oxidative stress in the brain. Consequently, propofol MCT/LCT could be particularly useful in adjusting levels of anesthesia in cases of ROS-induced brain disease.

Nitroxyl spin probes are usually eliminated by a combination of excretion *via* the kidney and bioreduction to the hydroxyl amine. The rate of elimination by the kidney seems to follow the usual pharmacologic pattern for the excretion of drugs, with those that tend to stay in the vascular system being excreted rapidly.[46] By contrast, neutral water-soluble nitroxyl spin probes, exhibiting an intermediate rate of urinary excretion, and lipophilic nitroxyl spin probes, such as MC-PROXYL used in this study (fig. 6), exhibit much reduced excretion *via* the kidney.[46,47] We have already confirmed that the metabolism of MC-PROXYL in the brain can be divided into phase I (vascular system) and phase II (reduced excretion *via* kidney), according to a two-compartment model of distribution using *in vivo* L-band ESR analysis.[21,22] Although several possible mechanisms should be considered to be responsible for the increased signal decay, a number of studies of L-bands in living animals have been associated with redox state, metabolism, and biologically relevant free radical generation.[48–53] Recently, it was shown that oxygen concentration, antioxidant content, and free radicals alter the signal decay rate of nitroxyl radical.[46,49] In the current study, we first measured the decay rate constant of the phase I component, which was dependent on bioreduction by the vascular system, of MC-PROXYL metabolism in the brain using the L-band ESR technique (fig. 6). Metabolism was probably in phase I because of the presence of ascorbate, which is a strong reducing agent of nitroxyl spin probes in the vascular system of the brain.[46] Therefore, we investigated the effects of propofol MCT/LCT on CBF, which is known to influence the bioreduction of MC-PROXYL in the blood circulation of the brain, in WKYs and SHRSPs. CBF in both WKYs and SHRSPs was immediately reduced by propofol MCT/LCT treatment. There were no significant differences in CBF level when compared between WKYs and SHPSPs 10 min after the injection of propofol MCT/LCT, a time period equivalent to the L-band ESR study (fig. 7). Therefore, results suggested that CBF is not likely to affect the bioreduction of MC-PROXYL in the brain of either WKYs or SHRSPs. The decay rate constant of MC-PROXYL was recovered when animals were anesthetized with propofol MCT/LCT but not pentobarbital (fig. 6). Collectively, this suggests that propofol MCT/LCT could reduce high oxidative stress in the brain of the SHRSP, a valued pathologic model of ischemic brain injury such as stroke.

If we turn our attention to how our results may relate to the clinic, it is important to consider the relative dose levels of the treatments used in the current study. The smallest concentration of propofol used was 10–30 μM, compared with the minimum concentration of propofol MCT/LCT of 56.09 μM used in our *in vitro* experiments (figs. 1–4). However, the scavenging effects of low concentrations of propofol MCT/LCT ($<$ 112.18 μM) were observed to be dependent on the effects of vehicle (fig. 1C), in a manner similar to that of propofol LCT (fig. 3). Brain tissue harvested from SHRSPs is known to exhibit high levels of oxidative stress.[21,22,28,29] Our current study has shown that propofol MCT/LCT treatment resulted in the recovery of normal levels of oxidative stress in the brain of SHRSPs (figs. 6 and 7). These results suggest the possibility that propofol MCT/LCT may exhibit useful antioxidant activity for clinical anesthesia for surgical aspects of brain disease such as craniotomy. However, further studies will be required to examine the clinical importance of propofol MCT/LCT, especially the MCT/LCT vehicle, on anesthesia in cases of ROS-induced brain disease.

In conclusion, our studies have demonstrated that propofol MCT/LCT and vehicle exhibits antioxidant properties by scavenging $HO^{\cdot}$ and can reduce high oxidative stress in the brain of SHRSPs. This suggests that propofol MCT/LCT can prevent ROS-related injuries in the brain, such as stroke, and thereby provide significant advantage for neuroprotection during anesthesia for craniotomy in patients with brain disease.

The authors thank Hirohisa Arakawa, D.D.S., Ph.D. (Professor, Department of Health Science Division of Oral Health, Kanagawa Dental College, Yokosuka, Kanagawa, Japan), for statistical advice.

References

1. Chan PH: Role of oxidants in ischemic brain damage. Stroke 1996; 27: 1124–9
2. Cobbs CS, Levi DS, Aldape K, Israel MA: Manganese superoxide dismutase expression in human central nervous system tumors. Cancer Res 1996; 56: 3192–5
3. Stadtman ER: Protein oxidation and aging. Science 1992; 257:1220–4
4. Rosen DR, Siddique T, Patterson D, Figlewicz DA, Sapp P, Hentati A, Donaldson D, Goto J, O'Regan JP, Deng HX, Rahmani Z, Krizus A, McKenna-Yasek D, Cayabyab A, Gaston SM, Berger R, Tanzi RE, Halperin JJ, Herzfeldt B, Van den Bergh R, Hung WY, Bird T, Deng G, Mulder DW, Smyth C, Laing NG, Soriano E, Pericak-Vance MA, Haines J, Rouleau GA, Gusella JS, Horvitz HR, Brown RH Jr: Mutations in Cu/Zn superoxide dismutase gene are associated with familial amyotrophic lateral sclerosis. Nature 1993; 362:59–62
5. Smith MA, Harris PL, Sayre LM, Perry G: Iron accumulation in Alzheimer disease is a source of redox-generated free radicals. Proc Natl Acad Sci U S A 1997; 94:9866–8
6. Evans PH: Free radicals in brain metabolism and pathology. Br Med Bull 1993; 49:577–87
7. Wilson JX, Gelb AW: Free radicals, antioxidants, and neurologic injury: Possible relationship to cerebral protection by anesthetics. J Neurosurg Anesthesiol 2002; 14:66–79
8. Chikutei K, Oyama TM, Ishida S, Okano Y, Kobayashi M, Matsui H, Horimoto K, Nishimura Y, Ueno SY, Oyama Y: Propofol, an anesthetic possessing neuroprotective action against oxidative stress, promotes the process of cell death induced by H_2O_2 in rat thymocytes. Eur J Pharmacol 2006; 540:18–23
9. De La Cruz JP, Villalobos MA, Sedeno G, Sanchez De La Cuesta F: Effect of propofol on oxidative stress in an *in vitro* model of anoxia-reoxygenation in the rat brain. Brain Res 1998; 800:136–44
10. Engelhard K, Werner C, Hoffman WE, Matthes B, Blobner M, Kochs E: The effect of sevoflurane and propofol on cerebral neurotransmitter concentrations during cerebral ischemia in rats. Anesth Analg 2003; 97:1155–61
11. Adembri C, Venturi L, Tani A, Chiarugi A, Gramigni E, Cozzi A, Pancani T, De Gaudio RA, Pellegrini-Giampietro DE: Neuroprotective effects of propofol in models of cerebral ischemia: Inhibition of mitochondrial swelling as a possible mechanism. ANESTHESIOLOGY 2006; 104:80–9
12. De Cosmo G, Congedo E, Clemente A, Aceto P: Sedation in PACU: The role of propofol. Curr Drug Targets 2005; 6:741–4
13. Fulton B, Sorkin EM: Propofol: An overview of its pharmacology and a review of its clinical efficacy in intensive care sedation. Drugs 1995; 50:636–57
14. Barrientos-Vega R, Mar Sanchez-Soria M, Morales-Garcia C, Robas-Gomez A, Cuena-Boy R, Ayensa-Rincon A: Prolonged sedation of critically ill patients with midazolam or propofol: Impact on weaning and costs. Crit Care Med 1997; 25:33–40
15. Theilen HJ, Adam S, Albrecht MD, Ragaller M: Propofol in a medium- and long-chain triglyceride emulsion: Pharmacological characteristics and potential beneficial effects. Anesth Analg 2002; 95:923–9
16. Kevin LG, Novalija E, Stowe DF: Reactive oxygen species as mediators of cardiac injury and protection: The relevance to anesthesia practice. Anesth Analg 2005; 101:1275–87
17. Lee C, Miura K, Liu X, Zweier JL: Biphasic regulation of leukocyte superoxide generation by nitric oxide and peroxynitrite. J Biol Chem 2000; 275: 38965–72
18. Lee CI, Liu X, Zweier JL: Regulation of xanthine oxidase by nitric oxide and peroxynitrite. J Biol Chem 2000; 275:9369–76
19. Lee MC, Shoji H, Komatsu T, Yoshino F, Ohmori Y, Zweier JL: Inhibition of superoxide generation from fMLP-stimulated leukocytes by high concentrations of nitric oxide or peroxynitrite: Characterization by electron spin resonance spectroscopy. Redox Rep 2002; 7:271–5
20. Lee MC, Shoji H, Miyazaki H, Yoshino F, Hori N, Miyake S, Ikeda Y, Anzai K, Ozawa T: Measurement of oxidative stress in the rodent brain using computerized electron spin resonance tomography. Magn Reson Med Sci 2003; 2:79–84
21. Lee MC, Shoji H, Miyazaki H, Yoshino F, Hori N, Toyoda M, Ikeda Y, Anzai K, Ikota N, Ozawa T: Assessment of oxidative stress in the spontaneously hypertensive rat brain using electron spin resonance (ESR) imaging and *in vivo* L-band ESR. Hypertens Res 2004; 27:485–92
22. Miyazaki H, Shoji H, Lee MC: Measurement of oxidative stress in stroke-prone spontaneously hypertensive rat brain using *in vivo* electron spin resonance spectroscopy. Redox Rep 2002; 7:260–5
23. Kuppusamy P, Zweier JL: Cardiac applications of EPR imaging. NMR Biomed 2004; 17:226–39
24. Miura Y, Utsumi H, Hamada A: Effects of inspired oxygen concentration on *in vivo* redox reaction of nitroxide radicals in whole mice. Biochem Biophys Res Commun 1992; 182:1108–14
25. Takeshita K, Hamada A, Utsumi H: Mechanisms related to reduction of radical in mouse lung using an L-band ESR spectrometer. Free Radic Biol Med 1999; 26:951–60
26. Gomi F, Utsumi H, Hamada A, Matsuo M: Aging retards spin clearance from mouse brain and food restriction prevents its age-dependent retardation. Life Sci 1993; 52:2027–33
27. Miura Y, Ozawa T: Noninvasive study of radiation-induced oxidative damage using *in vivo* electron spin resonance. Free Radic Biol Med 2000; 28:854–9
28. Chen X, Touyz RM, Park JB, Schiffrin EL: Antioxidant effects of vitamins C and E are associated with altered activation of vascular NADPH oxidase and superoxide dismutase in stroke-prone SHR. Hypertension 2001; 38:606–11
29. Kishi T, Hirooka Y, Kimura Y, Ito K, Shimokawa H, Takeshita A: Increased reactive oxygen species in rostral ventrolateral medulla contribute to neural mechanisms of hypertension in stroke-prone spontaneously hypertensive rats. Circulation 2004; 109:2357–62
30. Lee C, Okabe E: Hydroxyl radical-mediated reduction of Ca^{2+}-ATPase activity of masseter muscle sarcoplasmic reticulum. Jpn J Pharmacol 1995; 67:21–8
31. Hagiwara T, Lee CI, Okabe E: Differential sensitivity to hydroxyl radicals of pre- and postjunctional neurovascular transmission in the isolated canine mesenteric vein. Neuropharmacology 2000; 39:1662–72
32. Sakurai K, Sasabe H, Koga T, Konishi T: Mechanism of hydroxyl radical scavenging by rebamipide: Identification of mono-hydroxylated rebamipide as a major reaction product. Free Radic Res 2004; 38:487–94
33. Ogasawara Y, Namai T, Yoshino F, Lee MC, Ishii K: Sialic acid is an essential moiety of mucin as a hydroxyl radical scavenger. FEBS Lett 2007; 581:2473–7
34. Field KJ, Lang CM: Hazards of urethane (ethyl carbamate): A review of the literature. Lab Anim 1988; 22:255–62
35. Field KJ, White WJ, Lang CM: Anaesthetic effects of chloral hydrate, pentobarbitone and urethane in adult male rats. Lab Anim 1993; 27:258–69
36. Buettner GR: Spin trapping: ESR parameters of spin adducts. Free Radic Biol Med 1987; 3:259–303
37. Petersen KD, Landsfeldt U, Cold GE, Petersen CB, Mau S, Hauerberg J, Holst P, Olsen KS: Intracranial pressure and cerebral hemodynamic in patients with cerebral tumors: A randomized prospective study of patients subjected to craniotomy in propofol–fentanyl, isoflurane–fentanyl, or sevoflurane–fentanyl anesthesia. ANESTHESIOLOGY 2003; 98:329–36
38. Kaisti KK, Langsjo JW, Aalto S, Oikonen V, Sipila H, Teras M, Hinkka S, Metsahonkala L, Scheinin H: Effects of sevoflurane, propofol, and adjunct nitrous oxide on regional cerebral blood flow, oxygen consumption, and blood volume in humans. ANESTHESIOLOGY 2003; 99:603–13
39. Engelhard K, Werner C, Eberspacher E, Pape M, Stegemann U, Kellermann K, Hollweck R, Hutzler P, Kochs E: Influence of propofol on neuronal damage and apoptotic factors after incomplete cerebral ischemia and reperfusion in rats: A long-term observation. ANESTHESIOLOGY 2004; 101:912–7
40. Yasuda T, Takahashi S, Matsuki A: Tumor necrosis factor-alpha reduces ketamine- and propofol-induced anesthesia time in rats. Anesth Analg 2002; 95:952–5
41. Kiyose M, Lee CI, Okabe E: Inhibition of skeletal sarcoplasmic reticulum Ca^{2+}-ATPase activity by deferoxamine nitroxide free radical. Chem Res Toxicol 1999; 12:137–43
42. Lee MC, Kawai Y, Shoji H, Yoshino F, Miyazaki H, Kato H, Suga M, Kubota E: Evidence of reactive oxygen species generation in synovial fluid from patients with temporomandibular disease by electron spin resonance spectroscopy. Redox Rep 2004; 9:331–6
43. Halliwell B: Oxidants and the central nervous system: Some fundamental questions. Is oxidant damage relevant to Parkinson's disease, Alzheimer's disease, traumatic injury or stroke? Acta Neurol Scand Suppl 1989; 126:23–33
44. Okamoto K, Yamamoto K, Morita N, Ohta Y, Chikugo T, Higashizawa T, Suzuki T: Establishment and use of the M strain of stroke-prone spontaneously hypertensive rat. J Hypertens Suppl 1986; 4:S21–4
45. Gemba T, Matsunaga K, Ueda M: Changes in extracellular concentration of amino acids in the hippocampus during cerebral ischemia in stroke-prone SHR, stroke-resistant SHR and normotensive rats. Neurosci Lett 1992; 135:184–8
46. Kochernginsky N, Swartz HM: Nitroxide Spin Labels: Reactions in Biology and Chemistry. Edited by Kochernginsky N, Swartz HM. Boca Raton, Florida, CRC Press, 1995, pp 27–66
47. Bacic G, Nilges MJ, Magin RL, Walczak T, Swartz HM: *In vivo* localized ESR spectroscopy reflecting metabolism. Magn Reson Med 1989; 10:266–72
48. Yokoyama H, Itoh O, Ogata T, Obara H, Ohya-Nishiguchi H, Kamada H: Temporal brain imaging by a rapid scan ESR-CT system in rats receiving intraperitoneal injection of a methyl ester nitroxide radical. Magn Reson Imaging 1997; 15:1079–84
49. Miura Y, Ozawa T: Noninvasive study of radiation-induced oxidative damage using *in vivo* electron spin resonance. Free Radic Biol Med 2000; 28:854–9
50. Miura Y, Utsumi H, Hamada A: Effects of inspired oxygen concentration on *in vivo* redox reaction of nitroxide radicals in whole mice. Biochem Biophys Res Commun 1992; 182:1108–14
51. Berliner LJ, Wan XM: *In vivo* pharmacokinetics by electron magnetic resonance spectroscopy. Magn Reson Med 1989; 9:430–4
52. Ishida S, Kumashiro H, Tsuchihashi N, Ogata T, Ono M, Kamada H, Yoshida E: *In vivo* analysis of nitroxide radicals injected into small animals by L-band ESR technique. Phys Med Biol 1989; 34:1317–23
53. Utsumi H, Muto E, Masuda S, Hamada A: *In vivo* ESR measurement of free radicals in whole mice. Biochem Biophys Res Commun 1990; 172:1342–8